Supplemental Material: Pressure dependent relaxation in the photo-excited Mott insulator ET-F_2TCNQ: influence of hopping and correlations on quasi-particle recombination rates

M. Mitrano[(1)], G. Cotugno[(1,2)], S.R. Clark[(3,2)], R. Singla[(1)], S. Kaiser[(1)], J. Staehler[(4)], R. Beyer[(5)], M. Dressel[(5)], L. Baldassarre[(6)], D. Nicoletti [(1)], A. Perucchi[(7)], T. Hasegawa[(8)], H. Okamoto[(9)], D. Jaksch[(2,3)], A. Cavalleri[(1,2)]

[(1)]*Max Planck Institute for the Structure and Dynamics of Matter, Luruper Chaussee 149, Hamburg, Germany*

[(2)] *Department of Physics, Oxford University, Clarendon Laboratory, Parks Road, Oxford, United Kingdom*

[(3)]*Centre for Quantum Technologies, National University of Singapore, Singapore*

[(4)]*Fritz Haber Institute of the Max Planck Society,* Faradayweg 4-6, 14195 Berlin, Germany

[(5)]*1. Physikalisches Insitut, Universität Stuttgart, Pfaffenwaldring 57, 70550 Stuttgart, Germany*

[(6)] *Center for Life NanoScience@Sapienza, Istituto Italiano di Tecnologia, V.le Regina Elena 291, Rome, Italy*

[(7)] *INSTM UdR Trieste-ST and Elettra - Sincrotrone Trieste S.C.p.A., S.S. 14 km 163.5 in Area Science Park, 34012 Basovizza, Trieste Italy*

[(8)]*National Institute of advanced Industrial Science and Technology, Tsukuba, Japan*

[(9)]*Department of Advanced material Science, University of Tokyo, Chiba 277-8561, Japan*

A. Determination of the steady state optical constants under pressure

1) Experimental details

The equilibrium infrared measurements were performed with two different setups, one located in the University of Stuttgart (Germany), the other in the beamline SISSI at the Elettra Synchrotron Radiation Facility of Trieste (Italy). All the measurements were performed at room temperature and in quasi-normal incidence conditions with linearly polarized light along the crystalline *a* axis.

In the first setup, infrared reflectivity spectra up to 1.1 GPa were collected with a piston-cylinder cell coupled to a Bruker IFS66v interferometer (diamond window diameter 3 mm). The hydrostatic medium chosen in that case was Daphne 7373 oil, and internal pressure has been monitored through the external applied pressure. In order to have a reliable indication of the internal pressure a preliminary calibration with the ruby fluorescence method [1] has been performed.

The second setup was based on a screw-diamond anvil cell (600 μm culet size) coupled to a Bruker Vertex70 interferometer through a Hyperion microscope equipped with Schwarzchild objectives [2]. Here both reflectivity and transmittance spectra were collected for each pressure point up to 2.0 GPa. The hydrostatic medium chosen for these measurements was CsI powder. Pressure was measured in-situ with the standard ruby fluorescence method [1]. Details about the referencing of the spectra are given in Ref. [2].

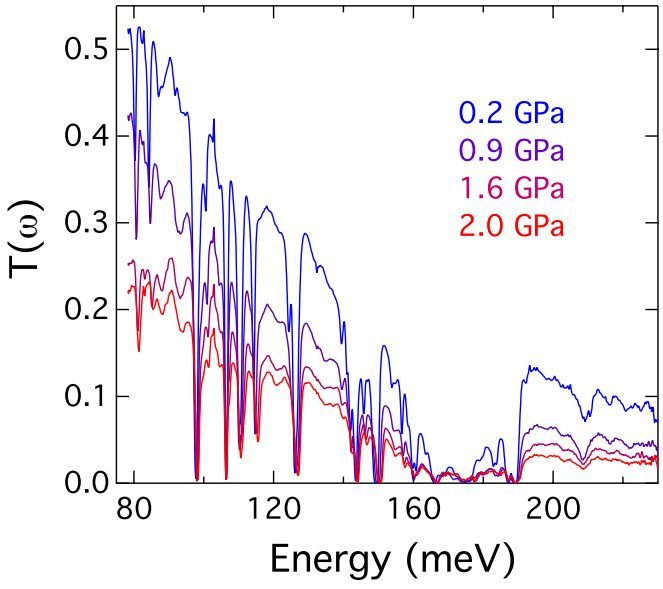

Fig. S1 – Steady state mid-infrared transmittance of ET-F_2TCNQ along the a axis for selected pressures.

2) Mid-infrared Transmittance

In order to reliably extract the optical conductivity of the ET-F_2TCNQ samples, we complement our reflectivity measurements by following the pressure dependence of the transmittance of a thin (10 μm) slab of sample in the mid-infrared region. Figure S1 shows the transmittance data for selected pressures. For energies above 240 meV the presence of the diamond anvil absorption prevents a reliable measurement of the transmittance .

3) Determination of the optical conductivity

In a diamond anvil cell the measurement of the reflectivity in the mid-infrared region is challenging because of the similarity of the refractive indices of the sample (n=2.60) and of the diamond anvil (n=2.37). Therefore the determination of the pressure dependent optical conductivities for the ET-F_2TCNQ is performed through a simultaneous Drude-Lorentz (DL) fit [2] of both the reflectivity and transmittance data for each pressure point.

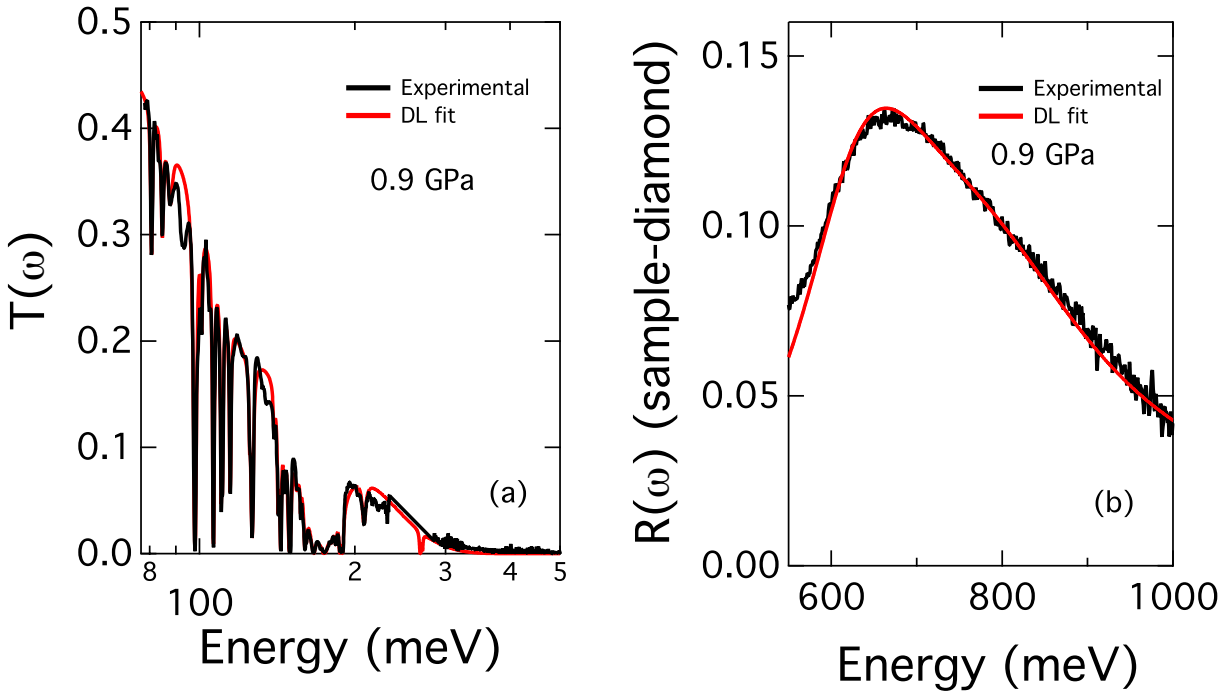

Fig. S2 – Sample Drude-Lorentz (DL) fit for the steady state mid-infrared transmittance and near-infrared reflectivity of the ET-F_2TCNQ along the a axis (at 0.9 GPa).

In detail, a Kramers-Kronig consistent DL fit is made on the transmittance for energies up to 300 meV, while for higher energies (up to 1000 meV) the reflectivity is fitted (see Fig. S2).

From the DL fit of the transmittance data, the low frequency part of the bulk reflectivity is then recalculated at the sample-diamond interface and merged with the experimental data above the multiphonon diamond absorption (namely above 550 meV).

The obtained full-range reflectivity at the sample-diamond interface is then used to calculate the optical conductivity $\sigma_1(\omega)$ through a standard Kramers-Kronig algorithm for samples in contact with a transmittive window [3]. The β parameter for the Kramers-Kronig transformation is kept fixed at 471 meV by checking the consistency of the output $\sigma_1(\omega)$ with the ambient pressure data where the Kramers-Kronig procedure is independent from this parameter. The merged reflectivities and the corresponding optical conductivities are reported in Fig. 1(c) – (d) of the main text.

B. Steady state theory fit of the optical conductivity

In the limit of large $U \gg t, V$ it is possible to analyze the extended Hubbard model by means of a $1/U$ expansion [4]. If we ignore corrections of order t/U then electron transfers are limited to those which conserve the number of doublons and in the ground state all sites are singly occupied. In this limit spin and charge dynamics decouple, leading to spin-charge separation, and a simple upper and lower Hubbard band picture emerges for the charges. The spin-dependence of the optical conductivity then enters only via a momentum dependent ground-state spin correlation g_q. This is further simplified by using the so-called "no-recoil approximation" where the dominant contributions to the conductivity are argued to arise from $q = 0$ and $q = \pi$ transitions [4], where $g_0 = 2.65$ and $g_\pi = 0.05$. The reduced optical conductivity is then given by

$$\omega\sigma_1(\omega) = \pi g_\pi t^2 e^2 \delta(\omega - \omega_2)$$
$$+ g_0 t^2 e^2 \left\{ \Theta(V - 2t)\pi \left(1 - \frac{4t^2}{V^2}\right)\delta(\omega - \omega_1) \right.$$
$$\left. + \Theta(4t - |\omega - U|) \frac{2t\sqrt{1 - \left(\omega - U/4t\right)^2}}{V(\omega - \omega_1)} \right\},$$

where $\Theta(x)$ is the Heaviside step function, $\omega_1 = U - V - 4t^2/V$ is the exciton energy and $\omega_2 = U - V$. The two δ peaks correspond to two different Mott-Hubbard excitons, with the $\Theta(V - 2t)$ factor expressing that the ω_1 exciton exists only when $V > 2t$. Owing to the small value of g_π the ω_2 exciton was ignored in our analysis due to its negligible weight. The final term is a semi-elliptic contribution from the particle-hole continuum which exists only for $|\omega - U| \leq 4t$. To allow comparison to the experiment the sharp features arising from the δ and Θ functions where convolved with a Lorentzian inducing a broadening $\eta \sim 2t$. The subsequent best-fit focused on the features near the CT resonance and provided the changes in the microscopic parameters displayed in Fig. 2(e) of the main text.

C. High-energy spinless fermion model

In the strong coupling limit it's possible to obtain an a simple effective Hamiltonian that describes the high-energy physics associated with particle-hole excitations across the Mott gap. This is achieved by first splitting the hopping terms into parts, one which conserves the number of double occupancies and one which does not. Following a well-known procedure [5], one seeks a canonical transformation S, which removes the order t non-conserving contributions. Retaining only the lowest order terms in t after this transformation then yields an effective Hamiltonian where the number of double occupations is a good quantum number. The non-conserving terms are now of order $\sim t^2/U$ and can be neglected in the strong-coupling limit $U \gg t$.

Exact eigenstates of this effective model can be found [6]. This is accomplished by defining spinless fermionic operators $\hat{a}_j$ for each site j which act only on the occupation indices $\vec{n} \equiv (n_1, \ldots, n_N)$, where

$n_j = 0$ or 1 counts the number of particles at site *j*. Charge excitations of the system can then be shown to be described by a Hamiltonian

$$H_{exc} = (U - V)\sum_j \hat{n}_j\hat{n}_{j+1} - t\sum_j \left(\hat{a}_j^+\hat{a}_{j+1} + \hat{a}_{j+1}^+\hat{a}_j\right),$$

where $\hat{n}_j = \hat{a}_j^+\hat{a}_j$ is the number operator. In the subspace of a single holon-doublon pair a convenient basis for the description of these charge excitations (or excitons) is in terms of a centre-of-mass coordinate *R,* and a relative coordinate *r*. This has the form

$$|\Psi_{HD}\rangle = \sum_{rR} \Phi(r,R)|R + r/2, R - r/2\rangle,$$

where $\left|R + \frac{r}{2}, R - \frac{r}{2}\right\rangle = \hat{a}_{R+r/2}^+\hat{a}_{R-r/2}^+|0\rangle$ with $|0\rangle$ being the vacuum of the two-body problem. The exciton is a two-particle bound state, so one looks for a solution in analogy to the hydrogen atom. The scalar product $\langle R + \frac{r}{2}, R - \frac{r}{2}|H_{exc}|\Psi_{HD}\rangle$ gives a difference equation for the exciton wavefunction [7]. Without loss of generality we can take the centre-of-mass momentum K to be $K = 0$ and the Schrödinger equation becomes

$$2t[2\,\psi_n(r) - \psi_n(r-a) - \psi_n(r+a)] - 4t\psi_n(r) - V\,\delta_{ra} + U\,\psi_n(r) = E\psi_n(r).$$

This is equivalent to single particle effective Hamiltonian defined on a semi-infinite tight-binding chain

$$H_{hd} = (U - V)|0\rangle\langle 0| + U\sum_{l=1}^{L}|l\rangle\langle l| - 2t\sum_{l=0}^{L-1}(|l\rangle\langle l+1| + |l+1\rangle\langle l|).$$

In Fig. 5 of the main text this effective model is depicted for L sites with open boundary conditions. The ground state configuration $|g\rangle$ signifying no holon-doublon pair has zero potential energy, while the adjacent holon-doublon configuration $|0\rangle$ has a potential energy $U - V$, and all the more distant holon-doublon configurations $|l\rangle$, where $l = 1,2,3,\cdots L$ have a potential energy U. The hopping between neighbouring holon-doublon configurations, e.g. $|l-1\rangle$ and $|l\rangle$, is included, but no hopping occurs between $|g\rangle$ and $|0\rangle$ because the coherent evolution in this strong-coupling limit conserves the

holon and doublon. Note that the hopping amplitude is $2t$ because the model describes the relative motion and the reduced effective mass of holon-doublon pair is half that of either excitation individually.

The current operator in this picture reduces to $J \propto |g\rangle\langle 0| + |0\rangle\langle g|$ which mimics the optical excitation of the Mott insulating ground state $|g\rangle$ through the creation of an adjacent (bound) holon-doublon configuration $|0\rangle$. The optical conductivity of the model $\sigma_1(z) = \langle g|J(z-H)^{-1}J|g\rangle$ is then equivalent to the single-particle Green function $G(z) = \langle 0|(z-H)^{-1}|0\rangle$, with complex frequency z. In the limit $L \to \infty$ this is found to be

$$G(z) = \frac{2}{z - U + 2V \pm \sqrt{(z-U)^2 - (4t)^2}}.$$

Expanding the imaginary part of $\omega\, G(\omega)$ and extracting the residue of the poles reproduces the dominant ω_1 Mott-Hubbard exciton δ peak and the particle-hole continuum found from the strong-coupling result in Eq. (2) in the main text. In other words, apart from the spin-averaging numerical factor g_0, the same spectral features of the extended Hubbard model in the limit $U \gg V, t$ are in fact captured by this simple effective model. Crucially the $2t$ hopping amplitude for the relative motion is responsible for the $8t$ bandwidth of the particle-hole continuum.

D. Spin-boson scaling of holon-doublon decay

To model holon-doublon recombination we apply a generic, but well-established description based on the celebrated spin-boson model [8]. Specifically, we consider focus on the ground state $|g\rangle$ and adjacent holon-doublon configuration $|0\rangle$ as a two-level system separated in energy by $U - V$. Then by coupling the electron density linearly to a continuum of bosonic modes the following spin-boson Hamiltonian is obtained

$$H_F = -t(|0\rangle\langle g| + |g\rangle\langle 0|) + (U-V)|0\rangle\langle 0| + \sum_n \lambda_n(\hat{b}_n^+ + \hat{b}_n)\,|0\rangle\langle 0| + \sum_n \omega_n \hat{b}_n^+ \hat{b}_n\,,$$

where $\hat{b}_n$ are the bosonic annihilation operators of the bath. The environment is completely characterised by the spectral function $\mathcal{J}(\omega) = \pi \sum_n \lambda_n^2 \delta(\omega - \omega_n)$ which combines the frequencies of the oscillators ω_n and their couplings λ_n. It can be related to the classical reorganization energy associated to the energy relaxation of a sudden electronic transition. This way of modelling a fluctuating dynamical polarization of the environment has found numerous applications to electron transfer problems [9,10].

Solutions of the spin-boson problem can in general display non-Markovian properties [11], dependent on the spectral function. We do not have precise knowledge of $\mathcal{J}(\omega)$ but can reasonably approximate it as having the form $\mathcal{J}(\omega) \propto \omega^s e^{-\omega/\omega_c}$, which for the most relevant electron-phonon interactions to intra- or inter-molecular vibrations is likely to be super-ohmic [12] with $s > 1$ and have a cut-off frequency obeying $U - V > \omega_c > t$. The bath is therefore non-adiabatic with respect to the hopping. Furthermore, the energy gap $U - V \gg t$ means that the model operates in the "large-bias" regime. In this limit the dynamics of the spin-boson model gives the decay rate Γ for an initial state $|0\rangle$ to decay to $|g\rangle$ by dissipation into the environment as [8]

$$\Gamma = \frac{1}{2}\left(\frac{t}{U-V}\right)^2 \mathcal{J}(U-V).$$

Only the value of the spectral function at the bias energy $U - V$ to be dissipated is relevant. Since this is above the cut-off the closest high frequency modes are intra-molecular vibrations which are likely to be unaffected by pressure to leading order. We therefore assume that the (unknown) value of $\mathcal{J}(U - V)$ is pressure independent and predict that the recombination rate scales with pressure via the dependent coherent parameters t and V as

$$\frac{\Gamma(P)}{\Gamma(0)} = \left(\frac{t(P)}{t(0)}\right)^2 \left(\frac{U - V(0)}{U - V(P)}\right)^2, \tag{S1}$$

after assuming that U is also independent of pressure. This scaling of the rate sensibly encodes an increase in the decay rate Γ with increasing hopping t, which is the process ultimately responsible for recombination, and an increase with decreasing bias $U - V$ between the levels.

E. Master equation for holon-doublon recombination

The super-ohmic and large-bias regime of the spin-boson model is known to exhibit overdamped behaviour [8]. Consequently non-Markovian memory effects, such as recurrences and oscillations in the populations due to back-action of the environment [13], are highly suppressed and its transient behaviour rapidly settles to the Markovian decay. The dynamics of the large-bias super-ohmic regime is therefore effectively Markovian [14] (although not necessarily weak-coupling). Moreover the experimentally measured short-time decay of the reflectivity shown in Fig. 3 of the main text, which is an approximate measure of the carrier density, displays a monotonic profile that is highly indicative of a Markovian process. Based on these observations we account for recombination in the strong-coupling limit effective model by introducing a local Markovian quantum dissipation process which incoherently drives $|0\rangle \rightarrow |g\rangle$. This is described by a Lindblad master equation [15] describing the evolution of the density matrix ρ as (taking $\hbar = 1$)

$$\frac{d}{d\tau}\rho(\tau) = -i[H, \rho(\tau)] + \Gamma\left(C\rho(\tau)C^{\dagger} - \tfrac{1}{2}C^{\dagger}C\rho(\tau) - \tfrac{1}{2}\rho(\tau)C^{\dagger}C\right),$$

where $C = |g\rangle\langle 0|$ is the jump operator. The resulting dynamics of the initial photo-excited state [16] $\rho(0) = |0\rangle\langle 0|$ then describes the competition between this local dissipation of a bound holon-doublon and the coherent evolution which acts to unbind the pair. We then numerically computed the population $n_g(\tau) = tr(\rho(\tau)|g\rangle\langle g|)$ in the ground state as a function of time up to 4 ps and found it was well fitted with a trial function $n_g(\tau) = A\left(1 - e^{-\Gamma_{eff}\tau}\right)$ allowing a determination of the effective quasi-particle decay rate $\Gamma_{eff} < \Gamma$. To predict the pressure dependence we first fitted the bare rate $\Gamma(0)$ so that $\Gamma_{eff}(0)$ equalled the experimental value for zero pressure. From this we used the spin-boson scaling in Eq. (S1) to determine $\Gamma(P)$ for all other pressure values from which the numerical solution of the model gave $\Gamma_{eff}(P)$. In Fig. 4 of the main text $\Gamma_{eff}(P)$ is shown for evolution computed by using $L = 20$ to model the particle-hole continuum.

REFERENCES

[1] H. K. Mao, J. Xu, and P. M. Bell, J. Geophys. Res. **91,** 4673 (1986)

[2] A. Perucchi, L. Baldassarre, P. Postorino and S. Lupi, J. Phys.: Condens. Matter **21,** 323202 (2009)

[3] J. S. Plaskett and P. N. Schatz, J. Chem. Phys. **38**, 612 (1963)

[4] F. H. L. Essler *et al.*, Phys. Rev. B **64**, 125119 (2001)

[5] S. K. Lyo, and J. P. Gallinar, J. Phys. C **10**, 1693 (1977); S. K. Lyo, Phys. Rev. B **18**, 1854 (1978); F. Gebhard, K. Born, M. Scheidler, P. Thomas, and S. W. Koch, Philos. Mag. Part B **75** 1-46 (1997)

[6] D. J. Klein, Phys. Rev. B **8**, 3452 (1973)

[7] W. Barford, *Electronic and Optical Properties of Conjugated Polymers* (Clarendon Press, Oxford, 2005)

[8] A. J. Leggett*,* S. Chakravarty, A. T. Dorsey, M. P. A. Fisher, A. Garg, W. Zwerger, Rev. Mod. Phys. **59**, 1 (1987)

[9] R. Egger, C.H. Mak and U. Weiss, J. Chem. Phys. **100**, 2651 (1994)

[10] S. Tornow, R. Bulla, F. B. Anders, A. Nitzan, Phys. Rev. B **78**, 035434 (2008)

[11] G. Clos and H.-P. Breuer, Phys. Rev. A **86**, 012115 (2012)

[12] U. Weiss, *Quantum Dissipative Systems*, 3rd ed. (World Scientific, 2008)

[13] P. Haikka, J.D. Cresser and S. Maniscalco, Phys. Rev. A **83**, 012112 (2011)

[14] A. Nazir, Phys. Rev. Lett. **103**, 146404 (2009); D.P.S. McCutcheon and A. Nazir, Phys. Rev. B **83**, 165101 (2011)

[15] H. J. Carmichael, *An Open System Approach to Quantum Optics Noise* (Springer, Berlin, 2005)

[16] E. Jeckelmann, Phys. Rev. B **67**, 075106 (2003)